JOURNAL OF VIROLOGY, Dec. 2005, p. 14614–14621 Vol. 79, No. 23
0022-538X/05/$08.00+0 doi:10.1128/JVI.79.23.14614–14621.2005
Copyright © 2005, American Society for Microbiology. All Rights Reserved.

ACE2 Receptor Expression and Severe Acute Respiratory Syndrome Coronavirus Infection Depend on Differentiation of Human Airway Epithelia

Hong Peng Jia,[1] Dwight C. Look,[2] Lei Shi,[2] Melissa Hickey,[1] Lecia Pewe,[1] Jason Netland,[1] Michael Farzan,[3] Christine Wohlford-Lenane,[1] Stanley Perlman,[1] and Paul B. McCray, Jr.[1]*

Departments of Pediatrics[1] and Internal Medicine,[2] Carver College of Medicine, University of Iowa, Iowa City, Iowa 52242, and Department of Microbiology and Molecular Genetics, Harvard University, Cambridge, Massachusetts 02138[3]

Received 16 June 2005/Accepted 14 September 2005

Studies of patients with severe acute respiratory syndrome (SARS) demonstrate that the respiratory tract is a major site of SARS-coronavirus (CoV) infection and disease morbidity. We studied host-pathogen interactions using native lung tissue and a model of well-differentiated cultures of primary human airway epithelia. Angiotensin converting enzyme 2 (ACE2), the receptor for both the SARS-CoV and the related human respiratory coronavirus NL63, was expressed in human airway epithelia as well as lung parenchyma. As assessed by immunofluorescence staining and membrane biotinylation, ACE2 protein was more abundantly expressed on the apical than the basolateral surface of polarized airway epithelia. Interestingly, ACE2 expression positively correlated with the differentiation state of epithelia. Undifferentiated cells expressing little ACE2 were poorly infected with SARS-CoV, while well-differentiated cells expressing more ACE2 were readily infected. Expression of ACE2 in poorly differentiated epithelia facilitated SARS spike (S) protein-pseudotyped virus entry. Consistent with the expression pattern of ACE2, the entry of SARS-CoV or a lentivirus pseudotyped with SARS-CoV S protein in differentiated epithelia was more efficient when applied to the apical surface. Furthermore, SARS-CoV replicated in polarized epithelia and preferentially exited via the apical surface. The results indicate that infection of human airway epithelia by SARS coronavirus correlates with the state of cell differentiation and ACE2 expression and localization. These findings have implications for understanding disease pathogenesis associated with SARS-CoV and NL63 infections.

Severe acute respiratory syndrome (SARS) emerged as a regional and global health threat in 2002–2003, resulting in approximately 800 deaths (5). An intense, cooperative worldwide effort rapidly led to the identification of the disease-causing agent as a novel SARS coronavirus (CoV) (18, 32) and the subsequent complete sequencing of the viral genome (24, 37). The SARS-CoV genome encodes 14 putative open reading frames encoding 28 potential proteins, and the functions of many of these proteins are not known. While the incidence of new cases of SARS waned in 2003–2004, many aspects of SARS disease pathogenesis and host-pathogen interactions remain unsolved.

Limited human pathological studies demonstrate that the respiratory tract is a major site of SARS-CoV infection and morbidity (8, 30). Two previously recognized human coronaviruses (HCoV-OC43 and HCoV-229E) cause ~30% of upper respiratory tract infections (14, 28), and, recently, two additional human coronaviruses, HCoV-NL63 (42) and HKU1 (46), were identified in association with bronchiolitis and pneumonia, respectively. Epidemiologic data suggest that infection with NL63 is common, as most adults have neutralizing antibodies to the virus (12). Limited studies of these other human coronaviruses indicate that they infect respiratory epithelia (2, 4, 44). Little is known regarding the initial steps of SARS-CoV interaction with the host cells in the respiratory tract, such as the cell types in which primary viral infection and replication occur. Viral RNA has been localized to cells of the conducting airways and alveoli by in situ hybridization in SARS postmortem samples (40). Experimental evidence in several animal models, including nonhuman primates (7, 19, 27, 38), mice (9, 13), ferrets (25), and Syrian hamsters (34) indicates that direct application of SARS-CoV to the respiratory tract results in pulmonary infection. Furthermore, epidemiologic analysis of a Toronto SARS outbreak supports the hypothesis that the virus is transmitted by respiratory droplets (49). Thus, it appears likely that interactions between SARS-CoV and respiratory epithelia play an important role in the genesis of SARS.

The cellular receptors mediating binding and entry have been identified for some coronaviruses associated with human disease. HCoV-229E uses CD13 as a receptor (48). The cellular receptors for HCoV-OC43 and HKU1 are currently unknown. Recently, angiotensin converting enzyme 2 (ACE2) was identified as a receptor for both SARS-CoV (21) and NL63 (12). ACE2 is a membrane-associated aminopeptidase expressed in vascular endothelia, renal and cardiovascular tissue, and epithelia of the small intestine and testes (6, 10, 11). A region of the extracellular portion of ACE2 that includes the first α-helix and lysine 353 and proximal residues of the N terminus of β-sheet 5 interacts with high affinity to the receptor binding domain of the SARS-CoV S glycoprotein (22).

Several unanswered questions remain regarding ACE2 expression in human respiratory epithelia and its role as a receptor for SARS-CoV. These include the identification of the

* Corresponding author. Mailing address: Department of Pediatrics, 240-G EMRB, Carver College of Medicine, University of Iowa, Iowa City, IA 52242. Phone: (319) 335-6844. Fax: (319) 335-6925. E-mail: paul-mccray@uiowa.edu.

Downloaded from http://jvi.asm.org/ on April 17, 2021 by guest

specific epithelial cell types expressing ACE2, the polarity of ACE2 expression, and whether SARS-CoV infection of respiratory epithelia is ACE2-dependent. Here we investigate interactions between SARS-CoV and human airway epithelia using native tissue and a primary culture model of polarized, well-differentiated tracheal and bronchial epithelia. Our findings indicate that the state of cell differentiation and ACE2 expression levels are both important determinants of the susceptibility of human airway epithelia to infection.

MATERIALS AND METHODS

Epithelial cell culture. Primary cultures of human airway epithelia were prepared from trachea or bronchi cells and grown at the air-liquid interface (ALI) on collagen-coated porous filters as described previously (17). In select experiments, the apical surface of primary cells was submerged under 500 μl of cell culture medium for 7 days to induce dedifferentiation or grown in nonpolarized fashion on tissue culture plastic. This study was approved by the Institutional Review Board at the University of Iowa. A549 cells (ATCC CCL-185) were maintained in Dulbecco's modified Eagle's medium/F12 (Gibco) containing 10% fetal bovine serum, penicillin (100 U/ml), and streptomycin (100 mg/ml).

Immunoblot analysis. Cells or tissues were lysed in 0.1% Triton X-100 in phosphate-buffered saline (PBS), and total protein was separated on a sodium dodecyl sulfate-7.5% polyacrylamide gel electrophoresis gel and transferred to polyvinylidene difluoride membrane. Goat anti-ACE2 polyclonal primary antibody (catalog no. AF933, R & D Systems, Minneapolis, MN), horseradish peroxidase-conjugated donkey anti-goat secondary antibody, mouse anti-foxj1 monoclonal primary antibody (gift of S. Brody, Washington University), and a horseradish peroxidase-conjugated goat anti-mouse secondary antibody were used. Primary antibody binding was visualized using SuperSignal chemiluminescent substrate (Pierce, Rockford, IL).

Immunofluorescence staining. Airway epithelia were fixed in 4% paraformaldehyde for 5 min at room temperature and washed with PBS. Five percent bovine serum albumin in PBS was used to block nonspecific antibody binding. An anti-ACE2 monoclonal antibody (MAB933; R & D Systems, Minneapolis, MN) was applied to cells (both apical and basolateral surfaces for air-liquid interface-cultured cells). Epithelia were then incubated at 37°C for 1 h and again washed with PBS. Rabbit anti-mouse fluorescein isothiocyanate-conjugated secondary antibody (F-4143; Sigma, St. Louis, MO) was added to cells and incubated at 4°C overnight. Cells were then washed with PBS, and a Cy3-labeled mouse anti-β-tubulin IV monoclonal antibody (C-4585; Sigma) was added. Cells were incubated at 37°C for 1 h, followed by PBS washes, and then mounted with DAPI (4′,6′-diamidino-2-phenylindole) VectaShield (Vector Labs, Burlingame, CA). Nuclei were stained with To-pro-3 (T3605; Sigma, St. Louis, MO). The SARS-CoV nsp1 protein was localized in cells fixed with 100% methanol using a rabbit polyclonal anti-nsp1 primary antibody (gift of M. Denison) (33) and a mouse anti-rabbit fluorescein isothiocyanate-conjugated secondary antibody (catalog no. A11088, Molecular Probes, Eugene, OR).

Surface biotinylation. The apical or basolateral surfaces of airway epithelia were treated with 1 mg/ml *N*-hydroxysulfosuccinimidobiotin (Pierce, Rockford, IL) in PBS for 30 min at 25°C. The epithelial surface was washed and then incubated with 100 mM glycine in PBS for 20 min at 25°C to quench unreacted biotin. Epithelial protein lysates were prepared by sonication in lysis buffer, and biotinylated proteins were precipitated using neutravidin covalently linked to immobilized diaminodipropylamine (Pierce). Biotinylated proteins were released in 8% sodium dodecyl sulfate-containing loading buffer, boiled, and analyzed by immunoblotting for ACE2. ErB2 was detected as a control basolateral membrane marker (43) using rabbit polyclonal anti-c-erbB2 antibody (Dako Corporation, Carpinteria, CA).

Scanning electron microscopy (SEM). Epithelia were fixed in 2.5% glutaraldehyde in Na cacodylate buffer for 30 min and rinsed with 0.1 M Na cacodylate buffer three times. Samples were postfixed in 1% OsO_4 for 1 h and sequentially rinsed with 0.1 M Na cacodylate buffer and H_2O. Samples were then serially dehydrated using 25% to 100% ethanol. After critical-point drying, samples were mounted on stubs, sputter coated, and examined using a Hitachi F-4000 electron microscope.

Real-time reverse transcription-PCR mRNA analysis. Total cellular RNA was isolated using TRI-Reagent (MRC, Cincinnati, OH) or a commercial spin column isolation kit (Stratagene, La Jolla, CA), and 1 μg was reverse transcribed using a reverse transcription (RT)-PCR kit (Ambion, Austin, TX). An aliquot of cDNA was subjected to PCR using an iCycler iQ fluorescence thermocycler (Bio-Rad, Hercules, CA) with SYBR green I DNA dye (Molecular Probes, Eugene, OR) and Platinum *Taq* DNA polymerase (iQ SYBR green Supermix kit, Bio-Rad). PCR conditions included denaturation at 95°C for 3 min and then for 35 cycles of 94°C for 30 s, 60°C for 30 s, and 72°C for 30 s, followed by 5 min at 72°C for elongation. The following primers were used: (i) human ACE2 forward 5′-GGACCCAGGAAATGTTCAGA-3′ and reverse 5′-GGCTGCAGA AAGTGACATGA-3′, (ii) SARS-CoV N gene forward/leader 5′-ATATTAGGT TTTTACCCAGG-3′ and reverse 5′-CTTGCCCCATTGCGTCCTCC-3′, (iii) SARS-CoV S gene forward/leader 5′-ATATTAGGTTTTTACCCAGG-3′ and reverse 5′-CTCCTGAGGGAACAACCCTG-3′, and (iv) human hypoxanthine phosphoribosyltransferase (HPRT) forward 5′-CCTCATGGACTGATTATG GAC-3′ and reverse 5′-CAGATTCAACTTGCGCTCATC-3′. Fluorescence data was captured during the 10-s dwell to ensure that primer dimers were not contributing to the fluorescence signal, and specificity of the amplification was confirmed using melting curve analysis. Data was collected and recorded by iCycler iQ software (Bio-Rad) and initially determined as a function of threshold cycle (C_T). Levels of mRNA were expressed relative to control HPRT levels, which were calculated as $2^{\Delta CT}$. In some samples, PCR products were visualized on 2% agarose gels with ethidium bromide.

Adenoviral vectors. E1-deleted replication incompetent adenoviral vectors expressing human ACE2, *Escherichia coli* β-galactosidase, and foxj1 under the control of the cytomegalovirus promoter were produced as previously described (1).

Preparation of SARS S protein-pseudotyped lentivirus and infection of airway epithelia. The SARS-CoV S protein cDNA (Urbani strain "S-H2," as described reference 21) was used to pseudotype feline immunodeficiency virus (FIV) expressing a nuclear-targeted β-galactosidase by using previously described methods (45). The virus was concentrated 250-fold by centrifugation, and titers were determined on HT1080 cells, obtaining titers of $\sim 2 \times 10^5$ to 4×10^6 transducing units/ml. Well-differentiated human airway epithelia were transduced with the pseudotyped FIV by applying 100 μl of solution to the apical surface of airway epithelia. After 1 h of incubation at 37°C, virus was removed and cells were incubated at 37°C for 2 days. To infect epithelia from the basolateral side, the Millicell insert was turned over, and virus was applied to the basolateral surface for 1 h in 100 μl of medium. Following the 1-h infection, virus was removed and the insert was turned upright and incubated at 37°C in 5% CO_2 for 2 days.

β-Galactosidase activity assays. The Galacto-Light chemiluminescent reporter assay (Tropix, Bedford, MA) was used to quantify β-galactosidase activity following the manufacturer's protocol. Relative light units were quantified using a luminometer (Monolight 3010; Pharmingen, San Diego, CA) and standardized to total protein in the sample.

Preparation of wild-type SARS-CoV and infection of airway epithelia. SARS-CoV (Urbani strain) was produced in Vero E6 cells under BSL3 containment conditions. Virus titers were determined on Vero E6 cells with typical yields of $\sim 4 \times 10^6$ PFU/ml. Epithelia derived from three donors were infected in duplicate with SARS-CoV from the apical surface (multiplicity of infection [MOI], 0.8). Following a 30-min incubation at 37°C, virus was removed and 10 washes with PBS were performed. A sample was collected by adding and removing 500 μl of medium from the apical side of one epithelium from each donor. A total of 500 μl of medium was added to the basolateral side of the remaining epithelia, and 24 h later, samples were collected for titer determinations.

RESULTS

ACE2 expression in human airway epithelia. ACE2 serves as the SARS-CoV receptor, at least for tissue culture cell entry (21). To determine if ACE2 is also the SARS-CoV receptor in the respiratory tract, we first looked for evidence of ACE2 protein expression in human lung tissue by Western blotting. An immunoreactive band consistent with the glycosylated form of ACE2 was identified in lysates from human airway and distal lung tissue (Fig. 1A). However, the cell type expressing ACE2 could not be identified in this experiment, as both endothelial and epithelial cells can express ACE2. Accordingly, we next evaluated ACE2 protein expression in well-differentiated primary cultures of airway epithelia using immunohistochemistry and observed airway epithelial cell expression, with the most abundant signal for ACE2 on the apical rather than the basolateral surface (Fig. 1B). Furthermore, the signal intensity was strongest on ciliated cells, as demonstrated by colocalization

Downloaded from http://jvi.asm.org/ on April 17, 2021 by guest

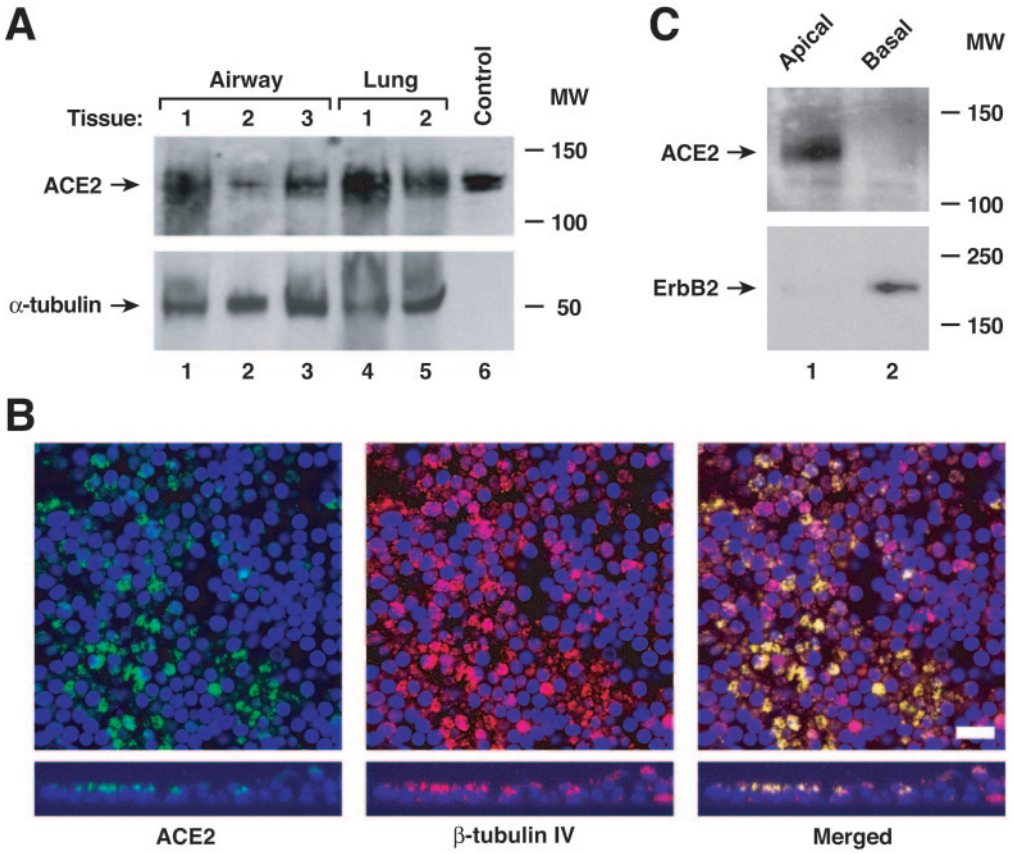

FIG. 1. ACE2 is expressed on human airway epithelia. (A) ACE2 protein levels were determined using immunoblot analysis of extracts from human airway and alveolar tissue. The control is recombinant ACE2 released into the supernatant from A549 cells infected with an adenoviral vector expressing human ACE2. The positions of ACE2 and α-tubulin are indicated by arrows. MW, molecular weight in thousands. (B) ACE2 protein location in polarized human airway epithelia was determined using immunofluorescence staining for ACE2 (green), β-tubulin IV (red), and nuclear DAPI (blue). Confocal fluorescence photomicroscopic images are presented en face (top) and from vertical sections (bottom). Colocalization is shown by yellow in the merged images. Bar, 10 μm. (C) ACE2 protein location in polarized human airway epithelia was determined by selective apical or basolateral biotinylation, immunoprecipitation of biotinylated surface proteins, and immunoblot analysis for ACE2 or control basolateral erbB2. MW, molecular weight in thousands. The positions of ACE2 and erbB2 are indicated by arrows.

with the β-tubulin IV marker of cilia (23), suggesting that ciliated cells express ACE2 abundantly. To confirm a polar distribution of ACE2 in differentiated epithelia, selective apical or basolateral surface biotinylation with subsequent precipitation was performed (Fig. 1C). Immunoblot analysis of precipitated proteins confirmed that ACE2 is expressed in greater abundance on the apical surface of conducting airway epithelia, although in some experiments a weak ACE2 signal was also detected basolaterally. In contrast, ErbB2, the receptor for heregulin-alpha, was more abundant on the basolateral surface as previously reported (43), confirming selective biotinylation.

Results from polarized epithelia suggested that ACE2 expression might depend on the state of cellular differentiation. To validate a model to test this hypothesis, we used SEM to compare the apical surface morphology of well-differentiated epithelia with that of well-differentiated cells subsequently grown with medium present on their apical surfaces for 7 days. Of note, submersion of the apical surfaces of primary cells caused loss of cilia (Fig. 2A). Loss of this important marker of cell differentiation with resubmersion was associated with markedly diminished expression of ACE2 mRNA and protein (Fig. 2B and C). In contrast to results in polarized epithelia, poorly differentiated primary human tracheobronchial epithelia (hTBE) or A549 cells grown on tissue culture plastic expressed little ACE2 mRNA or protein. Interestingly, foxj1, a transcription factor required for a well-differentiated ciliated epithelia phenotype (3) was also coordinately expressed with ACE2, indicating that ACE2 positively correlates with the state of epithelial differentiation. We also asked whether foxj1 might directly regulate ACE2 expression in airway epithelia. Primary tracheobronchial cells grown in submersion culture were transduced with an adenoviral vector expressing ACE2, a negative-control β-galactosidase, or foxj1. Only transduction with the ACE2 vector conferred ACE2 expression, suggesting that foxj1 expression alone does not regulate ACE2 (Fig. 2D and data not shown).

SARS-CoV infection of human airway epithelia. To evaluate the polarity of entry of the SARS-CoV in airway epithelia, we prepared FIV virions pseudotyped with SARS S protein. The ACE2 dependence of transduction with SARS S protein-pseudotyped FIV virions was first evaluated on 293 cells with or without cotransfection with human ACE2 cDNA. We ob-

Downloaded from http://jvi.asm.org/ on April 17, 2021 by guest

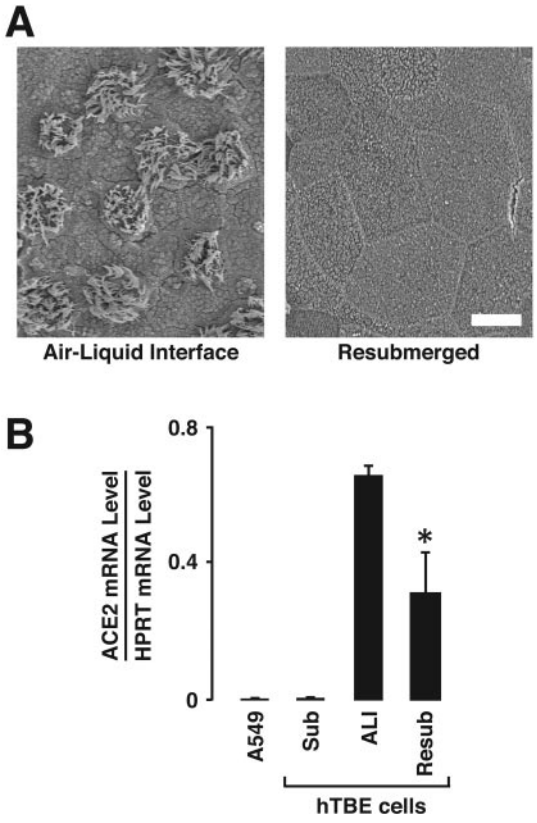

FIG. 2. ACE2 expression is associated with airway epithelial cell differentiation. (A) Ciliated epithelial cell differentiation in cultures of primary airway epithelial cells under air-liquid interface or resubmerged conditions was verified by SEM of the apical epithelial surface. Bar, 10 μm. (B) ACE2 mRNA levels were determined using real-time RT-PCR analysis of samples from A549 cells or primary hTBE cells cultured under undifferentiating submerged (Sub), differentiating ALI, or resubmerged (Resub) conditions. Values are expressed as mean mRNA levels relative to control HPRT mRNA levels plus or minus standard deviations (SD) ($n = 3$), and the asterisk indicates a significant difference in mRNA levels between air-liquid interface and resubmerged conditions. (C) ACE2 protein levels were determined using immunoblot analysis of extracts from A549 or primary hTBE cells. The positions of ACE2, foxj1 (to verify epithelial cell differentiation status), and β-actin are indicated by arrows. MW, molecular weight in thousands. (D) ACE2 protein levels were determined using immunoblot analysis of extracts from hTBE cells under submerged conditions that were infected with a recombinant adenoviral vector that expressed ACE2, control transgene (β-galactosidase), or foxj1. MW, molecular weight in thousands.

served that 293 cell transduction with this vector was almost completely ACE2-dependent (Fig. 3A). To establish the ACE2 dependence of human airway epithelia for SARS-CoV, we transduced poorly differentiated A549 cells and submerged primary hTBE cells that do not express constitutive ACE2 with increasing amounts of an adenoviral vector expressing human ACE2. After 48 h, SARS-CoV S protein-pseudotyped-FIV was applied to the apical surface at an MOI of 0.1 (based on HT1080 titers). There was an inoculum-dependent increase in the transduction of cells that expressed ACE2 (Fig. 3B). S protein-pseudotyped FIV was then used to contrast the efficiency of entry in A549 cells, poorly differentiated (submerged) human airway epithelia, and well-differentiated (ALI) epithelia. Only well-differentiated epithelial cells showed significant β-galactosidase expression following transduction (Fig. 3C). We next applied the pseudotyped virus to the apical or basolateral surfaces of well-differentiated primary cultures of human airway epithelia to investigate whether the virus preferentially entered from one cell surface. After 2 days, the cells were harvested and entry was evaluated by β-galactosidase activity. Transduction of human airway epithelia by the S protein-pseudotyped virions occurred more efficiently when applied from the apical rather than the basolateral surface (Fig. 3D). This pattern of entry correlates with ACE2 expression on polarized cells (Fig. 1). In contrast, FIV pseudotyped with the vesicular stomatitis virus-G envelope entered polarized cells better from the basolateral surface.

We went on to perform select experiments using wild-type SARS-CoV (Urbani strain). Using protocols similar to those outlined for Fig. 3, we evaluated the ability of SARS-CoV to infect multiple human airway epithelial cell culture models. Under BSL3 containment, we applied the virus to A549 cells, poorly differentiated (submerged) primary cultures of airway epithelia, or well-differentiated (ALI) human airway epithelia at an MOI of 0.8. A549 and hTBE cells cultured under submerged conditions expressed little detectable SARS-CoV N or S gene mRNA after infection (Fig. 4A). In contrast, in well-differentiated cells infected with SARS-CoV from the apical surface, the N and S gene mRNAs were detected at high levels. We confirmed that the gene products detected in real-time RT-PCR assays were generated from new SARS-CoV mRNA templates rather than viral genome by verifying the appropriate size of the amplified products (Fig. 4B). The primers used

Downloaded from http://jvi.asm.org/ on April 17, 2021 by guest

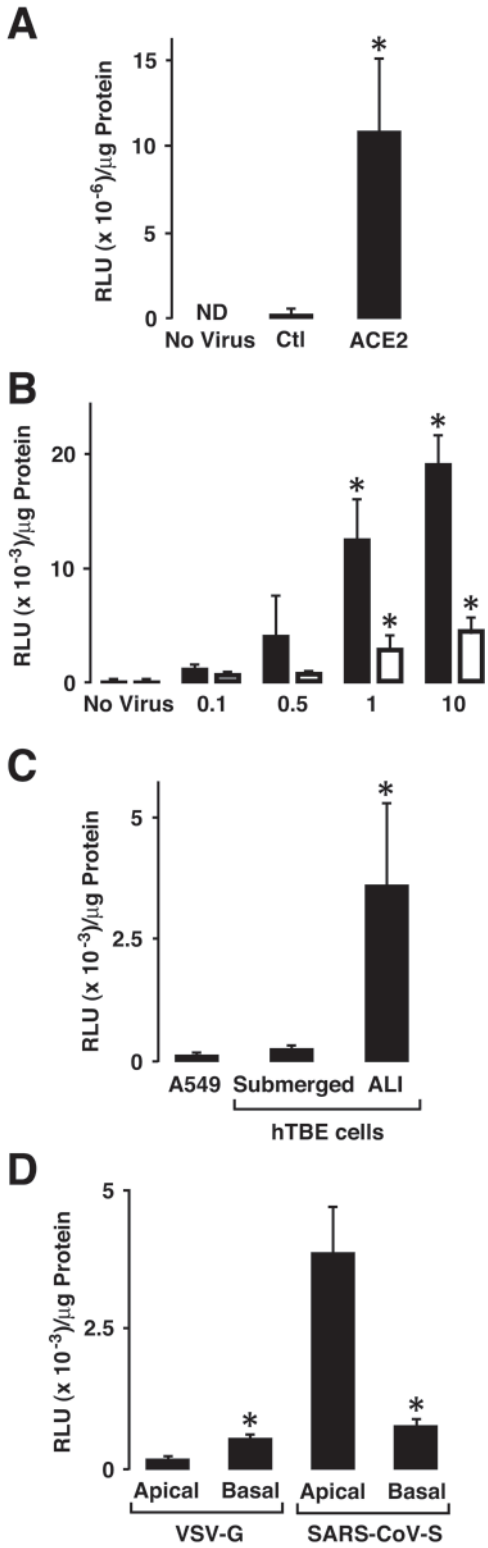

FIG. 3. SARS-CoV S protein-pseudotyped FIV infects differentiated airway epithelia best from the apical surface. (A) β-galactosidase levels were determined by enzyme activity in 293 cells transfected with a plasmid expressing control (Ctl) transgene or human ACE2 and then infected with SARS-S protein-pseudotyped FIV expressing β-galactosidase. ND, not detected. (B) β-galactosidase levels were determined in A549 cells (black bars) or primary hTBE cultured under submerged conditions (white bars) that were first infected with an adenoviral vector expressing ACE2 at the indicated MOI and then infected with SARS-S protein-pseudotyped FIV expressing β-galactosidase. (C) β-Galactosidase levels determined in extracts from A549 cells or primary hTBE cultured under submerged or ALI conditions that were infected from the apical surface with SARS-S protein-pseudotyped FIV expressing β-galactosidase. (D) β-galactosidase levels determined in primary hTBE cultured under ALI conditions that were infected from the apical or basolateral surface with vesicular stomatitis virus-G or SARS-S protein-pseudotyped FIV. In panels A through D, values are expressed as means plus or minus SD ($n = 4$ to 6) and a significant difference from levels on uninfected cells (A and B), hTBE cells cultured under submerged conditions (C), or cells infected from the apical surface (D) is indicated by an asterisk. RLU, relative light units.

included a forward primer in the conserved SARS CoV 5′ leader sequence and gene-specific reverse primers. These results suggest that SARS-CoV infects undifferentiated human airway epithelial cells poorly or not at all, while well-differentiated airway epithelia are susceptible.

To document that SARS-CoV productively infects human airway epithelia, we applied the virus to the apical surface of well-differentiated human airway epithelia at an MOI of ~0.8 for 30 min and then measured the release of virus 24 h later. As shown in Table 1, these results indicate that, following apical application of SARS-CoV, a productive infection occurred and virus was preferentially released apically. We confirmed SARS-CoV infection of polarized epithelia by immunostaining cells for the SARS-CoV nsp1 protein 24 h following infection. Confocal microscopy revealed viral nsp1 protein in the cytoplasm, consistent with replication complexes, following apical application of the virus (Fig. 4C). Control, noninfected cells showed no staining. The infection of permissive Vero E6 cells showed intense cytoplasmic staining only in the presence of SARS-CoV infection (data not shown). To better define the cell types infected by SARS-CoV in this model, we colocalized the nsp1 and β-tubulin IV proteins (Fig. 4D). Nsp1 staining was observed in perinuclear regions and distributed throughout the cytoplasm. In addition, we observed some areas of colocalization of nsp1 and β-tubulin IV, suggesting that replication complexes may assemble in the cytoplasm near or within cilia. These findings indicate that ciliated cells are the predominant cell type infected by SARS-CoV in well-differentiated airway epithelia.

DISCUSSION

We report the novel observation that SARS-CoV infection of human airway epithelia is dependent upon the state of epithelial differentiation and ACE2 mRNA and protein expression. ACE2 is more abundantly expressed on the apical surface of polarized epithelia, and we show for the first time that well-differentiated cells support viral replication with viral entry and egress occurring primarily from the apical surface. Thus, SARS-CoV preferentially infects well-differentiated ciliated epithelial cells expressing ACE2. Since ACE2 is also the receptor for the coronavirus NL63 (12), these findings are relevant to the biology of infection with this more common human pathogen.

ACE2 expression in human tissues correlates with known sites of infection, including lung and intestine (6, 10, 11). ACE2 is an ectoenzyme that converts angiotensin II to angio-

Downloaded from http://jvi.asm.org/ on April 17, 2021 by guest

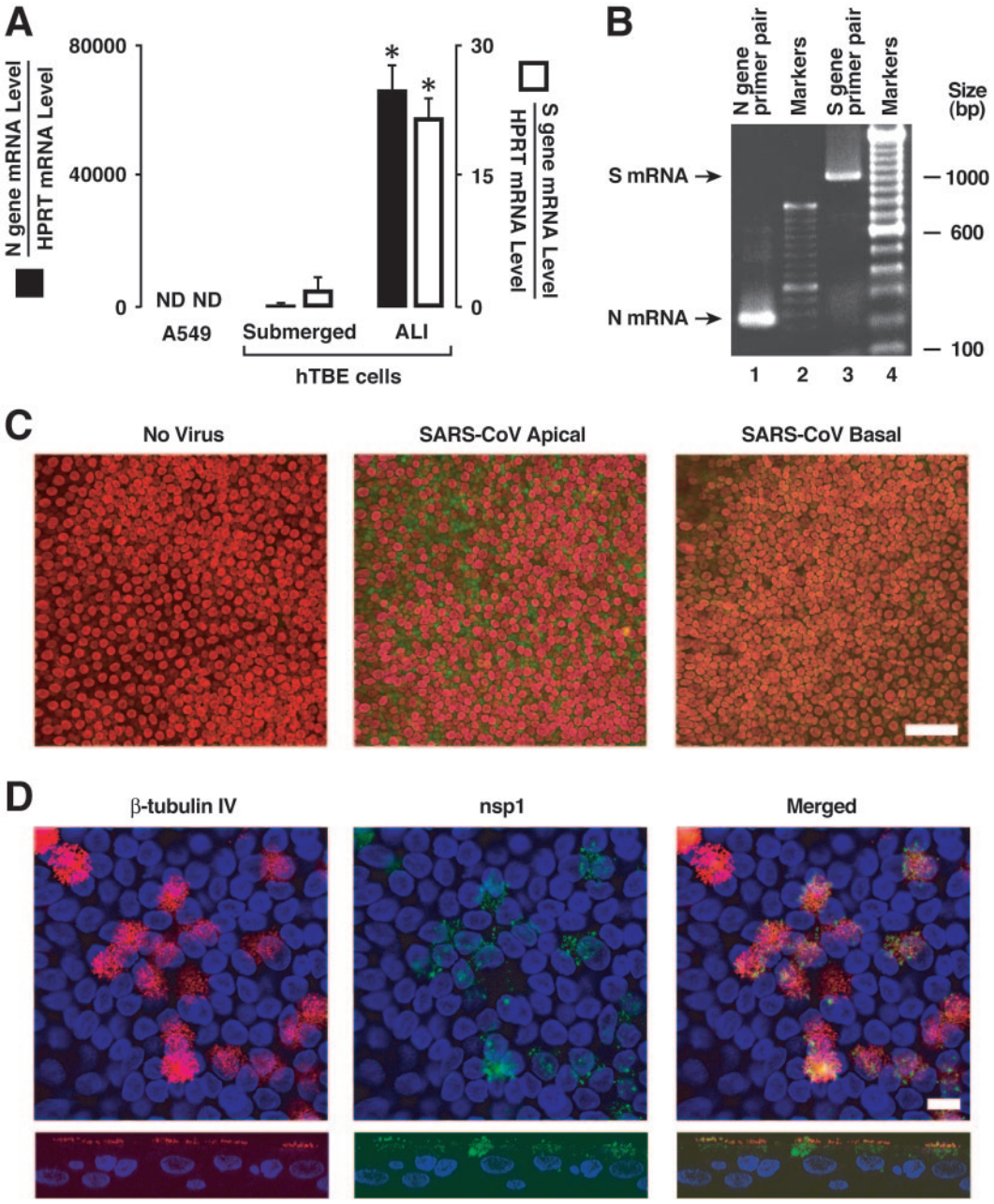

FIG. 4. Infection of differentiated airway epithelia by SARS-CoV. (A) SARS-CoV N and S gene mRNA levels were determined using real-time RT-PCR analysis of A549 cells or primary hTBE cultured under submerged or ALI conditions and infected with SARS-CoV from the apical surface at an MOI of 0.8 for 24 h. Values are expressed as mean mRNA levels relative to control HPRT mRNA levels plus or minus SD ($n = 2$). ND, not detected. An asterisk indicates a significant difference in mRNA levels between submerged and ALI conditions. (B) PCR products in panel A for hTBE cells cultured under ALI conditions were visualized by ethidium bromide. bp, base pairs. (C) SARS-CoV nsp1 replicase protein location in polarized human airway epithelia that were left uninfected or infected from the apical or basolateral side with SARS-CoV. Twenty-four hours following infection with SARS-CoV viral replication, complexes were localized using immunofluorescence staining for nsp1 (green) and nuclear To-pro-3 (red). Bar, 50 μm. (D) Colocalization of SARS-CoV nsp1 protein and cilia in polarized human airway epithelia. Airway epithelia were infected as described in the legend for Fig. 4C and then fixed and immunostained for nsp1 (green) or β-tubulin IV (red) as a marker for ciliated cells. The merged image shows colocalization of nsp1 and β-tubulin, indicating that the predominant infected cell types were ciliated epithelia. Bar, 10 μm.

tensin (1–7) (41), but its physiologic role in the airways is currently unknown. The predominant apical distribution of ACE2 suggests that the enzyme may be available to cleave peptides at the mucosal surface of the airway, but the native substrates in the lung have not yet been identified.

Epidemiologic data indicate that SARS-CoV is spread by respiratory droplets and contact (49). While such findings suggest that the virus enters the host through the mucosa of the respiratory tract and the eyes, many details of the initial steps of respiratory cell infection by SARS-CoV in humans are

Downloaded from http://jvi.asm.org/ on April 17, 2021 by guest

TABLE 1. Polar release of SARS-CoV following apical application to airway epithelia[a]

Virion egress type	Egress value (PFU/ml) for specimen no.:		
	1	2	3
Apical	2.5×10^4	5×10^4	3×10^4
Basolateral	15	20	5

[a] Urbani strain SARS-CoV at an MOI of 0.8 was applied to the apical surface of well-differentiated epithelia from three different human donors. Virion egress was assayed 24 h later by determining the titers for Vero E6 cells.

poorly understood. Limited human pathology data, primarily autopsy studies from SARS patients with severe disease and secondary complications, including respiratory failure, indicate the presence of virus in both proximal and distal pulmonary epithelia (40). Most data from human respiratory tissue from SARS patients was obtained two or more weeks following disease onset (8, 15, 20, 40). Lung tissue from such patients exhibits changes of diffuse alveolar damage, desquamated epithelial cells, type II cell hyperplasia, fibrin and collagen deposits in the alveolar space, increased mononuclear infiltrates in the interstitium, and, in some cases, the presence of multinucleated syncytial cells. Such changes reflect the combined effects of primary infection, host immune responses, and therapeutic interventions.

Human ACE2 appears necessary and sufficient to serve as a receptor for SARS-CoV (21). While both dendritic-cell-specific ICAM3-grabbing nonintegrin (DC-SIGN; CD209) and DC-SIGNR (L-SIGN, CD209L) can enhance SARS-CoV infection of ACE2 expressing cells, these proteins are not sufficient to support infection in the absence of ACE2 (16, 26, 47). Several recent reports using SARS-CoV or retroviral vectors pseudotyped with SARS S protein (31, 39, 47) (29) indicated that human airway epithelial cell lines were poorly transduced, an unexpected finding that raised questions regarding the ability of respiratory epithelia to support SARS-CoV infection. The present studies help explain these results. Since SARS-CoV infection of airway epithelia is ACE2-dependent, and ACE2 expression is greatest in well-differentiated cells, the low transduction efficiencies of nonpolarized, poorly differentiated cells are not unanticipated.

Our findings suggest that the epithelium of the conducting airways, the major site of respiratory droplet deposition, supports the replication of SARS-CoV. The observation that ACE2 complementation of poorly differentiated epithelia enhanced transduction with S protein-pseudotyped virions in a dose-dependent manner further supports its role as a receptor. In the setting of a productive infection of conducting airway epithelia, the apically released SARS-CoV might be removed by mucociliary clearance and gain access to the gastrointestinal tract. SARS-CoV infects cells in the gastrointestinal tract, and diarrhea is a clinical sign commonly observed in patients with SARS (5). Furthermore, the preferential apical exit pathway of virions would favor the spread of infection along the respiratory tract. While not a focus of this study, pathological data indicate that SARS-CoV infects type II pneumocytes (40). The infection and release of virus in this compartment with its close proximity to the pulmonary capillary bed might allow systemic spread of virus to distant organs, especially in the context of inflammation and alveolar capillary leak. This pattern of apical infection and release of virus in polarized epithelia is reminiscent of transmissible porcine gastroenteritis virus (36) and HCoV-229E (44). In contrast, mouse hepatitis virus-A59 enters polarized cells from the apical surfaces and exits from the basolateral side (35).

In summary, studies in models of human airway epithelial differentiation and polarity reveal that SARS-CoV infects well-differentiated cells from the apical surface and preferentially exits from the apical side. These findings should also apply to the entry of NL63 in human airway epithelia. ACE2 expression in airway epithelia appears to be both necessary and sufficient for SARS-CoV infection. Airway epithelial expression of ACE2 is dynamic and associated with cellular differentiation, a finding that may underlie susceptibility to infection. The apical expression of ACE2 on epithelia indicates that this coronavirus receptor is accessible for topical application of receptor antagonists or inhibitors. To date, the factors regulating ACE2 expression have not been identified. Future studies of the ACE2 promoter and gene expression associated with cell differentiation may reveal regulators of ACE2 expression and subsequent SARS-CoV and NL63 susceptibility.

ACKNOWLEDGMENTS

We acknowledge the support of NIH PO1 AI060699-01.

We thank Jian Shao and Paola Vermeer for technical advice and assistance. We thank Steve Brody for supplying the antibodies against foxj1, an adenoviral vector expressing foxj1, and helpful discussions. We thank Carmen Halabi and Curt Sigmund for providing the human ACE2 cDNA. We also acknowledge the support of the Cell Culture and Gene Transfer Vector Cores, partially supported by the Center for Gene Therapy for Cystic Fibrosis (NIH P30 DK-54759) and the Cystic Fibrosis Foundation, for preparing airway epithelial cultures and adenoviral vectors.

REFERENCES

1. **Anderson, R. D., R. E. Haskell, H. Xia, B. J. Roessler, and B. L. Davidson.** 2000. A simple method for the rapid generation of recombinant adenovirus vectors. Gene Ther. **7:**1034–1038.
2. **Bradburne, A. F., M. L. Bynoe, and D. A. Tyrrell.** 1967. Effects of a "new" human respiratory virus in volunteers. Br. Med. J. **3:**767–769.
3. **Brody, S. L., X. H. Yan, M. K. Wuerffel, S. K. Song, and S. D. Shapiro.** 2000. Ciliogenesis and left-right axis defects in forkhead factor HFH-4-null mice. Am. J. Respir. Cell Mol. Biol. **23:**45–51.
4. **Chilvers, M. A., M. McKean, A. Rutman, B. S. Myint, M. Silverman, and C. O'Callaghan.** 2001. The effects of coronavirus on human nasal ciliated respiratory epithelium. Eur. Respir. J. **18:**965–970.
5. **Donnelly, C. A., A. C. Ghani, G. M. Leung, A. J. Hedley, C. Fraser, S. Riley, L. J. Abu-Raddad, L. M. Ho, T. Q. Thach, P. Chau, K. P. Chan, T. H. Lam, L. Y. Tse, T. Tsang, S. H. Liu, J. H. Kong, E. M. Lau, N. M. Ferguson, and R. M. Anderson.** 2003. Epidemiological determinants of spread of causal agent of severe acute respiratory syndrome in Hong Kong. Lancet **361:**1761–1766.
6. **Donoghue, M., F. Hsieh, E. Baronas, K. Godbout, M. Gosselin, N. Stagliano, M. Donovan, B. Woolf, K. Robison, R. Jeyaseelan, R. E. Breitbart, and S. Acton.** 2000. A novel angiotensin-converting enzyme-related carboxypeptidase (ACE2) converts angiotensin I to angiotensin 1–9. Circ. Res. **87:**e1-e9. [Online.]
7. **Fouchier, R. A., T. Kuiken, M. Schutten, G. van Amerongen, G. J. van Doornum, B. G. van den Hoogen, M. Peiris, W. Lim, K. Stohr, and A. D. Osterhaus.** 2003. Aetiology: Koch's postulates fulfilled for SARS virus. Nature **423:**240.
8. **Franks, T. J., P. Y. Chong, P. Chui, J. R. Galvin, R. M. Lourens, A. H. Reid, E. Selbs, C. P. McEvoy, C. D. Hayden, J. Fukuoka, J. K. Taubenberger, and W. D. Travis.** 2003. Lung pathology of severe acute respiratory syndrome (SARS): a study of 8 autopsy cases from Singapore. Hum. Pathol. **34:**743–748.
9. **Glass, W. G., K. Subbarao, B. Murphy, and P. M. Murphy.** 2004. Mechanisms of host defense following severe acute respiratory syndrome-coronavirus (SARS-CoV) pulmonary infection of mice. J. Immunol. **173:**4030–4039.
10. **Hamming, I., W. Timens, M. L. Bulthuis, A. T. Lely, G. J. Navis, and H. van Goor.** 2004. Tissue distribution of ACE2 protein, the functional receptor for SARS coronavirus. A first step in understanding SARS pathogenesis. J. Pathol. **203:**631–637.

Downloaded from http://jvi.asm.org/ on April 17, 2021 by guest

11. **Harmer, D., M. Gilbert, R. Borman, and K. L. Clark.** 2002. Quantitative mRNA expression profiling of ACE 2, a novel homologue of angiotensin converting enzyme. FEBS Lett. **532:**107–110.
12. **Hofmann, H., P. Krzysztof, L. van der Hoek, M. Geier, B. Berkhout, and S. Pohlmann.** 2005. Human coronavirus NL63 employs the severe acute respiratory syndrome coronavirus receptor for cellular entry. Proc. Natl. Acad. Sci. USA **102:**7988–7993.
13. **Hogan, R. J., G. Gao, T. Rowe, P. Bell, D. Flieder, J. Paragas, G. P. Kobinger, N. A. Wivel, R. G. Crystal, J. Boyer, H. Feldmann, T. G. Voss, and J. M. Wilson.** 2004. Resolution of primary severe acute respiratory syndrome-associated coronavirus infection requires Stat1. J. Virol. **78:**11416–11421.
14. **Holmes, K. V., and M. M. C. Lai.** 1996. *Coronaviridae*: the viruses and their replication, p. 1075–1093. *In* B. N. Fields, D. M. Knipe, and P. M. Howley (ed.), Fields virology, 3rd ed. Lippincott-Raven Publishers, Philadelphia, Pa.
15. **Hwang, D. M., D. W. Chamberlain, S. M. Poutanen, D. E. Low, S. L. Asa, and J. Butany.** 2004. Pulmonary pathology of severe acute respiratory syndrome in Toronto. Mod. Pathol. **23:**23.
16. **Jeffers, S. A., S. M. Tusell, L. Gillim-Ross, E. M. Hemmila, J. E. Achenbach, G. J. Babcock, W. D. Thomas, Jr., L. B. Thackray, M. D. Young, R. J. Mason, D. M. Ambrosino, D. E. Wentworth, J. C. Demartini, and K. V. Holmes.** 2004. CD209L (L-SIGN) is a receptor for severe acute respiratory syndrome coronavirus. Proc. Natl. Acad. Sci. USA **101:**15748–15753. (First published 20 October 2004; 10.1073/pnas.0403812101.)
17. **Karp, P. H., T. O. Moninger, S. P. Weber, T. S. Nesselhauf, J. L. Launspach, J. Zabner, and M. J. Welsh.** 2002. An in vitro model of differentiated human airway epithelia. Methods for establishing primary cultures. Methods Mol. Biol. **188:**115–137.
18. **Ksiazek, T. G., D. Erdman, C. S. Goldsmith, S. R. Zaki, T. Peret, S. Emery, S. Tong, C. Urbani, J. A. Comer, W. Lim, P. E. Rollin, S. F. Dowell, A. E. Ling, C. D. Humphrey, W. J. Shieh, J. Guarner, C. D. Paddock, P. Rota, B. Fields, J. DeRisi, J. Y. Yang, N. Cox, J. M. Hughes, J. W. LeDuc, W. J. Bellini, and L. J. Anderson.** 2003. A novel coronavirus associated with severe acute respiratory syndrome. N. Engl. J. Med. **348:**1953–1966.
19. **Kuiken, T., R. A. Fouchier, M. Schutten, G. F. Rimmelzwaan, G. van Amerongen, D. van Riel, J. D. Laman, T. de Jong, G. van Doornum, W. Lim, A. E. Ling, P. K. Chan, J. S. Tam, M. C. Zambon, R. Gopal, C. Drosten, S. van der Werf, N. Escriou, J. C. Manuguerra, K. Stohr, J. S. Peiris, and A. D. Osterhaus.** 2003. Newly discovered coronavirus as the primary cause of severe acute respiratory syndrome. Lancet **362:**263–270.
20. **Lang, Z., L. Zhang, S. Zhang, X. Meng, J. Li, C. Song, L. Sun, and Y. Zhou.** 2003. Pathological study on severe acute respiratory syndrome. Chin. Med. J. (Engl.) **116:**976–980.
21. **Li, W., M. J. Moore, N. Vasilieva, J. Sui, S. K. Wong, M. A. Berne, M. Somasundaran, J. L. Sullivan, K. Luzuriaga, T. C. Greenough, H. Choe, and M. Farzan.** 2003. Angiotensin-converting enzyme 2 is a functional receptor for the SARS coronavirus. Nature **426:**450–454.
22. **Li, W., C. Zhang, J. Sui, J. H. Kuhn, M. J. Moore, S. Luo, S. K. Wong, I. C. Huang, K. Xu, N. Vasilieva, A. Murakami, Y. He, W. A. Marasco, Y. Guan, H. Choe, and M. Farzan.** 2005. Receptor and viral determinants of SARS-coronavirus adaptation to human ACE2. EMBO J. **24:**1634–1643.
23. **Look, D. C., M. J. Walter, M. R. Williamson, L. Pang, Y. You, J. N. Sreshta, J. E. Johnson, D. S. Zander, and S. L. Brody.** 2001. Effects of paramyxoviral infection on airway epithelial cell Foxj1 expression, ciliogenesis, and mucociliary function. Am. J. Pathol. **159:**2055–2069.
24. **Marra, M. A., S. J. Jones, C. R. Astell, R. A. Holt, A. Brooks-Wilson, Y. S. Butterfield, J. Khattra, J. K. Asano, S. A. Barber, S. Y. Chan, A. Cloutier, S. M. Coughlin, D. Freeman, N. Girn, O. L. Griffith, S. R. Leach, M. Mayo, H. McDonald, S. B. Montgomery, P. K. Pandoh, A. S. Petrescu, A. G. Robertson, J. E. Schein, A. Siddiqui, D. E. Smailus, J. M. Stott, G. S. Yang, F. Plummer, A. Andonov, H. Artsob, N. Bastien, K. Bernard, T. F. Booth, D. Bowness, M. Czub, M. Drebot, L. Fernando, R. Flick, M. Garbutt, M. Gray, A. Grolla, S. Jones, H. Feldmann, A. Meyers, A. Kabani, Y. Li, S. Normand, U. Stroher, G. A. Tipples, S. Tyler, R. Vogrig, D. Ward, B. Watson, R. C. Brunham, M. Krajden, M. Petric, D. M. Skowronski, C. Upton, and R. L. Roper.** 2003. The genome sequence of the SARS-associated coronavirus. Science **300:**1399–1404.
25. **Martina, B. E., B. L. Haagmans, T. Kuiken, R. A. Fouchier, G. F. Rimmelzwaan, G. Van Amerongen, J. S. Peiris, W. Lim, and A. D. Osterhaus.** 2003. Virology: SARS virus infection of cats and ferrets. Nature **425:**915.
26. **Marzi, A., T. Gramberg, G. Simmons, P. Moller, A. J. Rennekamp, M. Krumbiegel, M. Geier, J. Eisemann, N. Turza, B. Saunier, A. Steinkasserer, S. Becker, P. Bates, H. Hofmann, and S. Pohlmann.** 2004. DC-SIGN and DC-SIGNR interact with the glycoprotein of Marburg virus and the S protein of severe acute respiratory syndrome coronavirus. J. Virol. **78:**12090–12095.
27. **McAuliffe, J., L. Vogel, A. Roberts, G. Fahle, S. Fischer, W. J. Shieh, E. Butler, S. Zaki, M. St Claire, B. Murphy, and K. Subbarao.** 2004. Replication of SARS coronavirus administered into the respiratory tract of African Green, rhesus and cynomolgus monkeys. Virology **330:**8–15.
28. **McIntosh, K., R. K. Chao, H. E. Krause, R. Wasil, H. E. Mocega, and M. A. Mufson.** 1974. Coronavirus infection in acute lower respiratory tract disease of infants. J. Infect. Dis. **130:**502–507.
29. **Mossel, E. C., C. Huang, K. Narayanan, S. Makino, R. B. Tesh, and C. J. Peters.** 2005. Exogenous ACE2 expression allows refractory cell lines to support severe acute respiratory syndrome coronavirus replication. J. Virol. **79:**3846–3850.
30. **Nicholls, J. M., L. L. Poon, K. C. Lee, W. F. Ng, S. T. Lai, C. Y. Leung, C. M. Chu, P. K. Hui, K. L. Mak, W. Lim, K. W. Yan, K. H. Chan, N. C. Tsang, Y. Guan, K. Y. Yuen, and J. S. Peiris.** 2003. Lung pathology of fatal severe acute respiratory syndrome. Lancet **361:**1773–1778.
31. **Nie, Y., P. Wang, X. Shi, G. Wang, J. Chen, A. Zheng, W. Wang, Z. Wang, X. Qu, M. Luo, L. Tan, X. Song, X. Yin, M. Ding, and H. Deng.** 2004. Highly infectious SARS-CoV pseudotyped virus reveals the cell tropism and its correlation with receptor expression. Biochem. Biophys. Res. Commun. **321:**994–1000.
32. **Poutanen, S. M., D. E. Low, B. Henry, S. Finkelstein, D. Rose, K. Green, R. Tellier, R. Draker, D. Adachi, M. Ayers, A. K. Chan, D. M. Skowronski, I. Salit, A. E. Simor, A. S. Slutsky, P. W. Doyle, M. Krajden, M. Petric, R. C. Brunham, and A. J. McGeer.** 2003. Identification of severe acute respiratory syndrome in Canada. N. Engl. J. Med. **348:**1995–2005.
33. **Prentice, E., J. McAuliffe, X. Lu, K. Subbarao, and M. R. Denison.** 2004. Identification and characterization of severe acute respiratory syndrome coronavirus replicase proteins. J. Virol. **78:**9977–9986.
34. **Roberts, A., L. Vogel, J. Guarner, N. Hayes, B. Murphy, S. Zaki, and K. Subbarao.** 2005. Severe acute respiratory syndrome coronavirus infection of golden Syrian hamsters. J. Virol. **79:**503–511.
35. **Rossen, J. W., W. F. Voorhout, M. C. Horzinek, A. van der Ende, G. J. Strous, and P. J. Rottier.** 1995. MHV-A59 enters polarized murine epithelial cells through the apical surface but is released basolaterally. Virology **210:**54–66.
36. **Rossen, J. W. A., C. P. J. Bekker, W. F. Voorhout, G. J. A. M. Strous, A. van der Ende, and P. J. M. Rottier.** 1994. Entry and release of transmissible gastroenteritis coronavirus are restricted to apical surfaces of polarized epithelial cells. J. Virol. **68:**7966–7973.
37. **Rota, P. A., M. S. Oberste, S. S. Monroe, W. A. Nix, R. Campagnoli, J. P. Icenogle, S. Penaranda, B. Bankamp, K. Maher, M. H. Chen, S. Tong, A. Tamin, L. Lowe, M. Frace, J. L. DeRisi, Q. Chen, D. Wang, D. D. Erdman, T. C. Peret, C. Burns, T. G. Ksiazek, P. E. Rollin, A. Sanchez, S. Liffick, B. Holloway, J. Limor, K. McCaustland, M. Olsen-Rasmussen, R. Fouchier, S. Gunther, A. D. Osterhaus, C. Drosten, M. A. Pallansch, L. J. Anderson, and W. J. Bellini.** 2003. Characterization of a novel coronavirus associated with severe acute respiratory syndrome. Science **300:**1394–1399.
38. **Rowe, T., G. Gao, R. J. Hogan, R. G. Crystal, T. G. Voss, R. L. Grant, P. Bell, G. P. Kobinger, N. A. Wivel, and J. M. Wilson.** 2004. Macaque model for severe acute respiratory syndrome. J. Virol. **78:**11401–11404.
39. **Simmons, G., J. D. Reeves, A. J. Rennekamp, S. M. Amberg, A. J. Piefer, and P. Bates.** 2004. Characterization of severe acute respiratory syndrome-associated coronavirus (SARS-CoV) spike glycoprotein-mediated viral entry. Proc. Natl. Acad. Sci. USA **101:**4240–4245.
40. **To, K., J. H. Tong, P. K. Chan, F. W. Au, S. S. Chim, K. Allen Chan, J. L. Cheung, E. Y. Liu, G. M. Tse, A. W. Lo, Y. Dennis Lo, and H. Ng.** 2004. Tissue and cellular tropism of the coronavirus associated with severe acute respiratory syndrome: an in-situ hybridization study of fatal cases. J. Pathol. **202:**157–163.
41. **Turner, A. J., J. A. Hiscox, and N. M. Hooper.** 2004. ACE2: from vasopeptidase to SARS virus receptor. Trends Pharmacol. Sci. **25:**291–294.
42. **van der Hoek, L., K. Pyrc, M. F. Jebbink, W. Vermeulen-Oost, R. J. Berkhout, K. C. Wolthers, P. M. Wertheim-van Dillen, J. Kaandorp, J. Spaargaren, and B. Berkhout.** 2004. Identification of a new human coronavirus. Nat. Med. **10:**368–373.
43. **Vermeer, P. D., L. A. Einwalter, T. O. Moninger, T. Rokhlina, J. A. Kern, J. Zabner, and M. J. Welsh.** 2003. Segregation of receptor and ligand regulates activation of epithelial growth factor receptor. Nature **422:**322–326.
44. **Wang, G., C. Deering, M. Macke, J. Shao, R. Burns, D. M. Blau, K. V. Holmes, B. L. Davidson, S. Perlman, and P. B. McCray, Jr.** 2000. Human coronavirus 229E infects polarized airway epithelia from the apical surface. J. Virol. **74:**9234–9239.
45. **Wang, G., V. A. Slepushkin, J. Zabner, S. Keshavjee, J. C. Johnston, S. L. Sauter, D. J. Jolly, T. Dubensky, B. L. Davidson, and P. B. McCray, Jr.** 1999. Feline immunodeficiency virus vectors persistently transduce nondividing airway epithelia and correct the cystic fibrosis defect. J. Clin. Invest. **104:**R49–R56.
46. **Woo, P. C., S. K. Lau, C. M. Chu, K. H. Chan, H. W. Tsoi, Y. Huang, B. H. Wong, R. W. Poon, J. J. Cai, W. K. Luk, L. L. Poon, S. S. Wong, Y. Guan, J. S. Peiris, and K. Y. Yuen.** 2005. Characterization and complete genome sequence of a novel coronavirus, coronavirus HKU1, from patients with pneumonia. J. Virol. **79:**884–895.
47. **Yang, Z. Y., Y. Huang, L. Ganesh, K. Leung, W. P. Kong, O. Schwartz, K. Subbarao, and G. J. Nabel.** 2004. pH-dependent entry of severe acute respiratory syndrome coronavirus is mediated by the spike glycoprotein and enhanced by dendritic cell transfer through DC-SIGN. J. Virol. **78:**5642–5650.
48. **Yeager, C. L., R. A. Ashmun, R. K. Williams, C. B. Cardellichio, L. H. Shapiro, A. T. Look, and K. V. Holmes.** 1992. Human aminopeptidase N is a receptor for human coronavirus 229E. Nature **357:**420–422.
49. **Yu, I. T., Y. Li, T. W. Wong, W. Tam, A. T. Chan, J. H. Lee, D. Y. Leung, and T. Ho.** 2004. Evidence of airborne transmission of the severe acute respiratory syndrome virus. N. Engl. J. Med. **350:**1731–1739.

Downloaded from http://jvi.asm.org/ on April 17, 2021 by guest